Ceria embedded nanocomposite coating fabricated by plasma electrolytic oxidation on titanium

M. Aliofkhazraei [a, *], R. Shoja Gharabagh [a], M. Teimouri [b], M. Ahmadzadeh [a], Ghasem Barati Darband [a], H. Hasannejad [a]

[a] Department of Materials Science, Faculty of Engineering, Tarbiat Modares University, Tehran, P.O. Box: 14115-143, Iran
[b] Department of Materials Science and Engineering, University of Texas at Arlington, Arlington, TX 76019, USA

ABSTRACT

In this study, wear and corrosion behaviors of PEO coatings on Ti substrate were evaluated. Ceria nanoparticles were added into PEO electrolyte as suspention. Rare earth elements and compounds are through environmental friendly and effective compounds. Effect of Ceria nanoparticles and their concentration was evaluated using SEM, FTIR, EDS, potentiodynamic polarization, EIS and pin on disk tests. In morphological investigations, it was revealed that with addition of 25 gr/L ceria nanoparticles, pores become filled and lowest surface roughness was achieved in this concentration. Corrosion potential of coatings moves toward noble potentials with addition of ceria nanoparticles and also corrosion current density decreases. Wear rate of coatings also decreased with ceria nanoparticle addition, but optimum properties depend on surface conditions. Wear rate decrease from 3.4 µg/N.m to 0.7 µg/N m by addition of 25 gr/L ceria nanoparticles.

© 2016 Elsevier B.V. All rights reserved.

1. Introduction

There are many different coating methods for applying wear and corrosion resistant coatings on materials including, electrodeposition [1], laser cladding [2], thermal spray [3], physical vapor deposition (PVD) [4] and chemical vapor deposition (CVD) [5], conversion coatings [6]. Regarding each of these method's parameters, sublayer to be coated, coating's material, expected working conditions, and cost of every method has its own advantages and limitations.

Titanium and its alloys have diverse applications in many fields including biomaterials [7], aerospace [8], chemical resistant materials [9] in bulk form and some applications including photocatalysis [10] and electrocatalysis [11] because of its oxide (TiO$_2$) unique semiconductor properties. This oxide layer also plays an important role in mechanical, wear and bioactive applications. Adhesion of this coating achieved through conversion coating methods, such as Plasma Electrolytic Oxidation, is much higher and defines further applications of this materials [12].

PEO is a new method for fabricating oxide coatings on light metals such as Al, Mg and also Ti. Process of these coatings fabrication is accompanied by discharge on the surface, this phenomena not only changes some morphological and roughness properties of coatings, but also enables elements to participate in coatings from electrolyte. PEO coatings on Ti, mostly are employed for biomedical [13,14], corrosion resistant [15] or wear resistant [16] applications. Composition of coatings is changed through base metal composition and PEO electrolyte. Nanoparticles also have been introduced into PEO coatings on Ti substrates, including Si$_3$N$_4$ [17] and PTFE [18] for wear applications, hydroxyapatite [19] and ZrO$_2$ [20] for biocompatible applications, carbon nano tubes [12] and recently CeO$_2$ [21].

Rare earth elements and compounds are used in corrosion and wear resistant coatings for replacing chromate conversion coatings because of their environment friendly nature [22]. Their usage background in PEO coatings initiates from their presence as alloying element in base metal. These studies were mostly on Mg substrates for their superior creep resistance [23,24]. Addition of Cerium ions into electrolytes was investigated from nitrate based precursors [25]. Utilizing Ceria nanoparticles in electrolytes of PEO coatings has also been reported [26]. Also cerium containing conversion coatings on Mg alloys have been reported [27]. Even PEO

* Corresponding author.
E-mail addresses: khazraei@modares.ac.ir, maliofkh@gmail.com (M. Aliofkhazraei).

coatings are post-treated with cerium containing baths [28]. Multi-step and combination of methods have also been utilized to fabricate oxide coatings containing cerium oxide on metals [29,30].

Since ceria nanoparticles in PEO electrolyte can alter wear and corrosion properties of coatings and above mentioned reports have showed improvements in corrosion behavior of PEO coatings on magnesium and titanium alloys. Ceria nanoparticles were added into PEO electrolyte as suspensions to moreover study wear behavior of these samples, since both wear and corrosion behavior are functional characteristics of coatings and a general view on both of these characteristics has not been studied, this study has been performed to further investigate effect of ceria nanoparticle concentration on corrosion and wear characteristics of PEO coatings on CP-Ti.

2. Experimental procedure

CP Ti sheets with 0.5 mm thickness (Grade 2) were cut into 5×5 cm^2 pieces, abraded with abrasive SiC paper up to 1000 grid. 1 L solution of 5 gr/L three sodium phosphate (Na$_3$PO$_4 \cdot$12H$_2$O) (Merck Co) and 5 gr/L sodium carbonate (Na$_2$CO$_3$) (Merck Co) was used as base PEO electrolyte and three different contents of ceria nanoparticles (50 nm average size SIGMA- ALDRICH) was added to the electrolyte in order to fabricate a suspension of nanoparticles. The set up was equipped with a water-cooled stainless steel cathode and a magnetic stirrer was used to maintain the suspension uniformly stirred. PEO process was performed with a home-made DC power supply with constant current density of 100 mA/cm^2. A Mira Tescan SEM was utilized for morphology assessments. Pin on disc wear test was implemented to study wear properties according to ASTM G 99 standard. Pin was a 6 mm radius Co-WC and samples were discs with sliding distances of 1800 m. Surtronic-25 (Taylor-Habson) was utilized to assess surface roughness with 0.01 μm resolution. Corrosion and electrochemical tests were performed by EG&G 273A potentiostat/galvanostat Princeton Applied Research, three electrode cell with scan rate of 1 mv/s and from −0.1 V to 1.2 V vs SCE.

3. Results and discussion

3.1. Microstructure and coating composition

SEM micrographs of the samples coated in different concentrations of cerium oxide have been shown in different magnifications in Fig. 1. As it can be seen, there are many pores in surface morphology of the specimens at low magnifications and specimens coated without cerium oxide (Fig. 1A) and few cracks are present in the image. The origin of these pores is the gas liberation from the melts caused by the growth process of coating formation. It is believed that the pores do not penetrate into whole thickness of oxide layer [31]. This is while the source of cracks formation is the release of the tensions caused by the coating growth process [32]. The diameter of pores and their number have been decreased by adding cerium oxide nanoparticles in an electrolyte. As can be seen in Fig. 1(e and f), cerium oxide nanoparticles have entered into the pores, filled and closed them. As seen in Fig. 1(g–h), cerium oxide nanoparticles have been evenly distributed on the surface and the agglomeration of the particles can be observed in some zones. On average, the size of nanoparticles is 50 nm. Cerium oxide nanoparticles move toward anode and discharge channels and lead to filling the pores. Some researchers have suggested combining the cerium oxide nanoparticles with other compounds in these channels [33]. By adding more nanoparticles in an electrolyte, the size of pores is increased. This may be due to increase of electrical resistance, because the electrolytic plasma is a constant current process,

hence increasing the resistance culminate in rising of discharging voltage and accordingly the amount of pores is also increased [34,35]. By comparing the SEM micrographs, it can be concluded that porosity is lowest in the coating formed in solution containing 25 gr/L of ceria and even at high magnifications, only very few pores are observed. According to a study by Lim et al. [26], they concluded that some of the pores are partially filled by ceria nanoparticles owing to increasing the amount of cerium oxide in the electrolyte. They also concluded that with increase of ceria concentration in electrolyte, its concentration in the coating also increases. According to the conducted researches [31,36,37] the amount of cracks and micro-pores is decreased in the coating by increasing the content of nanoparticles in solution and surface becomes more uniform. Nanoparticles are existing not only on the surface but also within the oxide layer [31,38]. Preferred locations for the deposition of cerium oxide nanoparticles are defects rich of tension such as micro-pores or cracks. These nanoparticles fill the structural defects and decrease coating porosities [26]. In general, plasma electrolytic coating is composed of two layers with a porous layer and a dense layer. It has been reported that cerium oxide nanoparticles and zirconium oxide ones are not present in the dense layer and their existence has only proven in porous layer [38]. Matykina et al. [39] found that the presence of zirconium oxide nanoparticles effectively alter the microstructure of PEO coating. They also concluded that zirconia nanoparticles are being located in outer layer of the coating in dendritic form. Different sizes and distribution of the pores on the surface of coating is resulting from cerium oxide in the coating electrolyte [40].

Results of EDX analysis concerning the samples coated in the electrolyte containing 50 gr/L ceria has been shown in Fig. 2. As it is observed, cerium element has not been precisely determined in this graph that its reason is titanium high peaks or overlapping of titanium and cerium peaks. In order to do further studies of specimens in different concentrations of cerium oxide, FTIR analysis was also performed. The graph has been shown in Fig. 3. This graph represents a peak in 1260 cm^{-1} that implying the bond between oxygen and cerium [41]. This peak has not observed in the sample coated in solution without the presence of ceria nanoparticles. This analysis with SEM image proves existing ceria nanoparticles in the coating. Cerium oxide nanoparticles are not ionized in aqueous electrolyte. So, their presence in the coating cannot be due to the electrochemical reactions. Therefore, the presence of these nanoparticles in the coating could be due to the electrophoretic and rotation of the suspension. Presence of cerium oxide nanoparticles has been reported by Di et al. [21]. Lim et al. [26] reported that negative zeta potential of the ceria nanoparticles leads to negative surface charge of cerium nanoparticles. Negatively charged surface of ceria nanoparticles causes ceria nanoparticles to migration toward the anode and participation in the coating process. Also, there is another report that indicates negative zeta potential of zirconium oxide nanoparticles (−60 mV at pH = 13) lead to the presence of nanoparticles in the initial state in the coating formation [42].

Curve of surface roughness as a function of the nanoparticles concentration in the electrolyte are shown in Fig. 4. As can be seen, the results of surface roughness are in compliance with SEM micrographs. Nanoparticle-free sample has the highest surface roughness and roughness is reduced by adding nanoparticles into the electrolyte. Added to that, surface roughness is increased by rise of the concentration of nanoparticles in the electrolyte. The reason of fact can be analyzed so that by increasing the amount of nanoparticles up to 50 gr/L, ceria nanoparticles are not completely deposited in the micro-pores, and some of these nanoparticles adhere to surface and thus increases the surface roughness [21]. Formation of oxide layer with larger pores leading to increasing the surface with great roughness. These nanoparticles fill the valleys
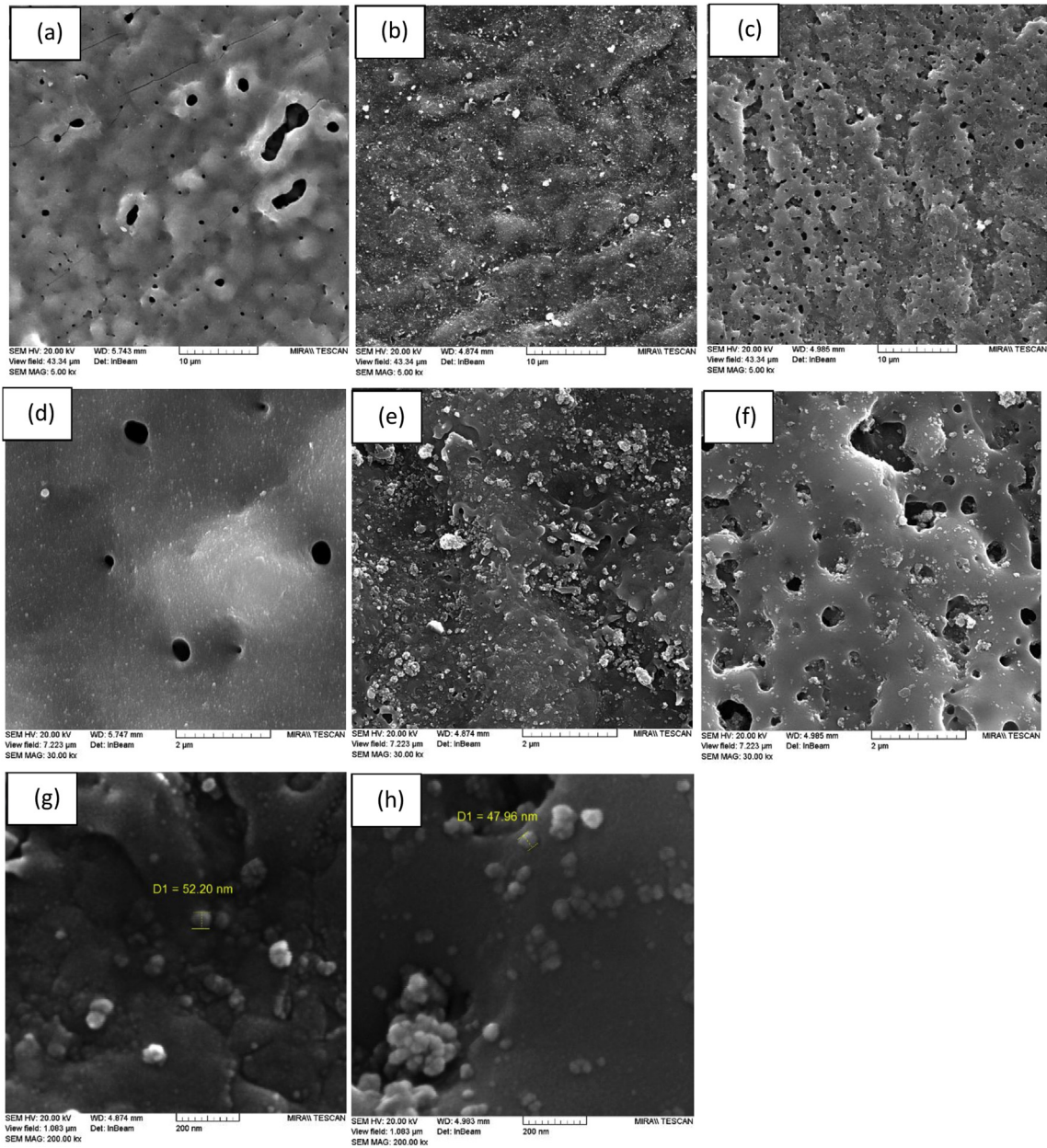
Fig. 1. Top surface SEM image of PEO coatings containing different concentrations of ceria nanoparticles at different magnification, (a–c, 5000×) a) 0 gr/L, b) 25 gr/L, c) 50 gr/L. (d–f, 30,000×) d) 0 g/L, e) 25 g/L, f) 50 g/L. (g–h, 2,00,000×) g) 25 g/L, h) 50 g/L.

and volcanic like structures of PEO coating layer, leading to reduce the height of the peaks and valleys. Therefore, the overall roughness of the surface is reduced by the presence of nanoparticles [43]. The results obtained from this study are consistent with those of Di et al. [21]. They concluded that by increasing the concentration of cerium oxide nanoparticles in the coating bath, surface roughness is decreased firstly and then increased.

3.2. Corrosion behavior of the coating

3.2.1. Potentiodynamic polarization test

Corrosion resistance of PEO coating was evaluated in various concentrations of ceria nanoparticles using potentiodynamic polarization test. Polarization curve of the samples coated in different concentrations of cerium oxide nanoparticles are shown in Fig. 5.

Corrosion current density, polarization resistance and corrosion potential are of important parameters in the evaluation of corrosion resistance. The results of the calculations of corrosion current density, polarization resistance and corrosion potential are given in Table 1.

As understood from extracted data of polarization curves in Table 1, corrosion current density has been decreased with addition of cerium oxide nanoparticles within the solution. This means reducing the corrosion rate, also the corrosion potential has been shifted toward more positive values which also means the reduction of coating corrosion tendency [26]. Increasing the corrosion resistance of PEO coatings due to the nanoparticles of aluminum oxide, titanium oxide and zirconium oxide has also been reported by other researchers [21]. As shown, the slope of anodic zone has been decreased with the addition of ceria nanoparticles within the
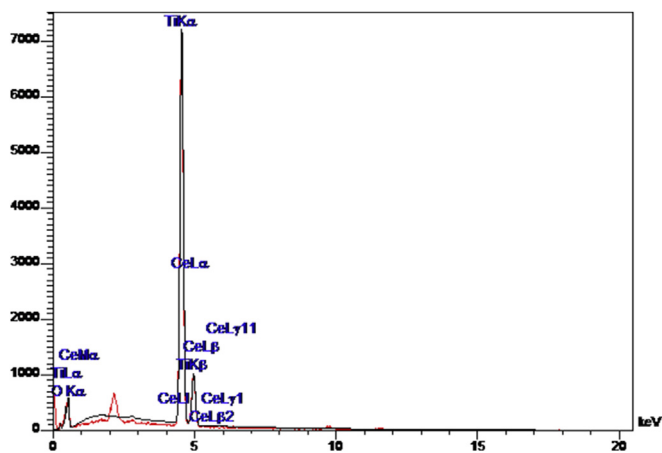
Fig. 2. EDX spectra of highest ceria concentration in PEO electrolyte (50 gr/L) sample.
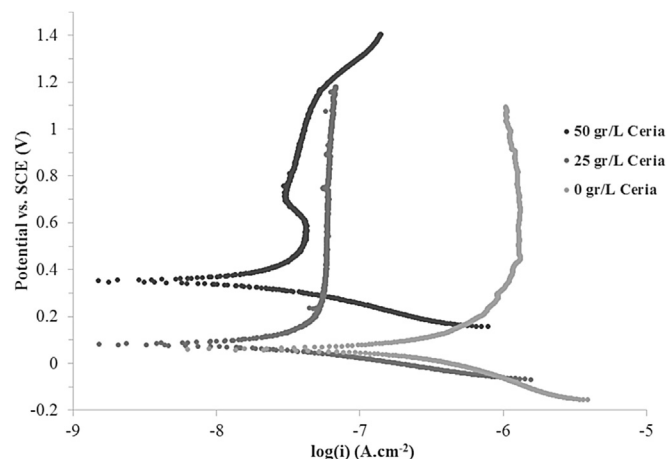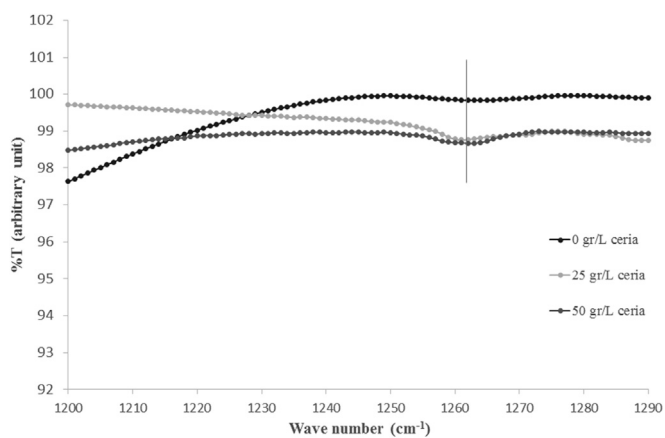

Fig. 3. FTIR spectra for samples with 0, 25 and 50 gr/L ceria nanoparticle concentration in projected view.
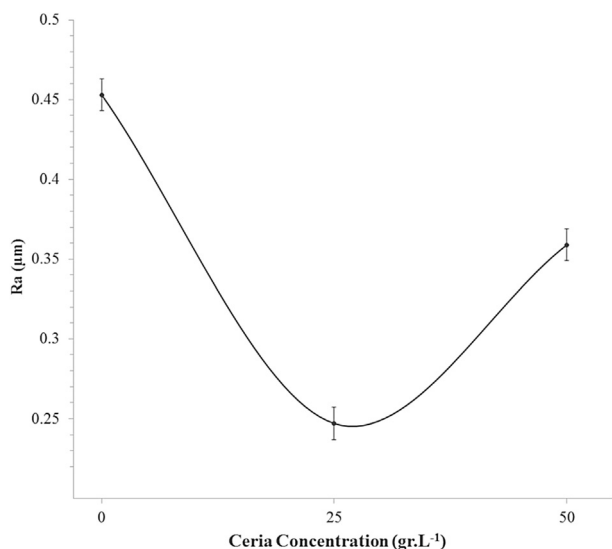

Fig. 4. Surface roughness of samples with different Ceria nanoparticle (0, 25, 50 gr/L).

coating which meant the reduction of kinetics of anodic reaction. Reducing the kinetics of anodic reaction means an overall reduction of reaction rate. Decrease of anodic reaction kinetics due to adding ceria nanoparticles has been also reported by Schem et al. [44].

Fig. 5. Potentiodynamic polarization curves of samples with different ceria concentration in PEO electrolyte.

Coating microstructure is one of the most important factors affecting the corrosion resistance of the coating. As it is seen from the SEM images, there were a lot of micro-pores on the sample surface in the coating with no cerium oxide. The presence of these micro-pores in the surface results in lowering corrosion resistance of the coating. When a sample is subjected to the electrolyte, the aggressive ions are penetrated into the coating through micro-pores and reaching to the interface between the layer and coating would reduce the corrosion resistance of the coating. As was observed, pores of the coating surface were filled by nanoparticles with addition of nanoparticles into the electrolyte which reduces the porosity and pores of the coating surface and it improves the corrosion resistance. Other factor affecting the corrosion resistance of the coating is surface roughness. Generally, it has been accepted that the surface having greater roughness is more susceptible to corrosion [45]. As it is observed, the amount of surface roughness was decreased by adding nanoparticles to the electrolyte, which this also improves the corrosion resistance of the coating. Higher polarization resistance of the coating containing cerium oxide reveals that the coating-substrate interface of the coating comprising cerium oxide nanoparticles acts as an appropriate barrier against penetration of corrosive ions; the reason can be due to higher chemical stability of the cerium oxide [46]. The reason of increasing corrosion resistance in the presence of cerium oxide nanoparticles can be firstly due to very high corrosion resistance of cerium oxide nanoparticles [47] and, secondly, to the amount of rutile phase [38]. Since the rutile is a phase resistant to corrosion, by increasing the amounts of rutile resulting from increasing the discharging temperature, corrosion resistance of the coating are being improved.

3.2.2. Electrochemical impedance spectroscopy

Electrochemical impedance spectroscopy test was also performed to obtain more information about corrosion behavior of the coating in different concentrations of cerium oxide nanoparticles. Nyquist and bode-phase plots correspondent to the specimens coated in different concentrations of nanoparticles is shown in Fig. 6.

The overall behavior of the Nyquist plot in the presence of cerium oxide nanoparticles are similar to previous reports. An equivalent circuit proposed for this curve has been shown in Fig. 7 in which R_S is solution resistance, R_{ct} charge transfer resistance for titanium double-layer, R_c PEO coating resistance, CPE_{ct} constant phase element of electric double-layer and CPE_c is constant phase element of PEO coating. Here a more general term of constant

Table 1
Linear Polarization Resistance extrapolation results of samples.

Ceria concentration (gr/L)	β_a (mV/dec)	β_c (mV/dec)	E_{corr}, vs SCE (mV)	i_{corr} (A cm^{-2})
0	86	158	60	1.41E-07
25	24	12	83	3.91E-09
50	27	38	353	3.96E-09
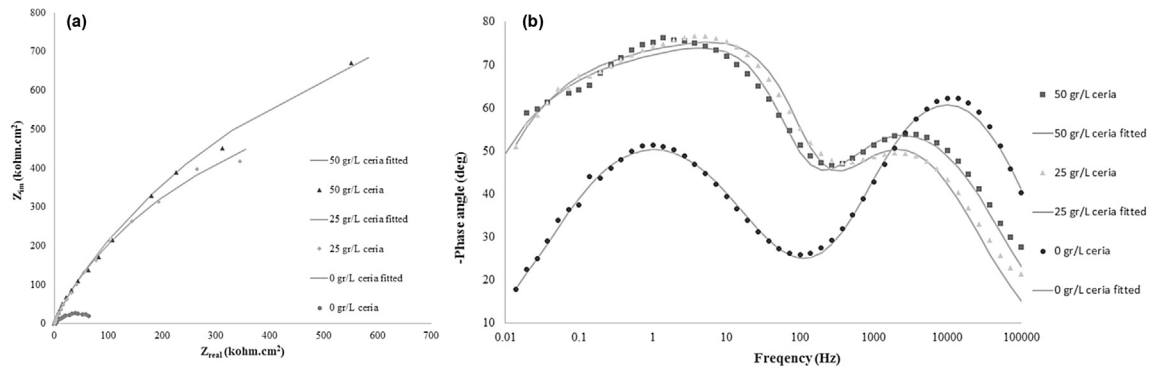
Fig. 6. Nyquist (a) and bode-phase (b) diagrams of samples coated in different concentrations of ceria nanoparticles and their fittings.
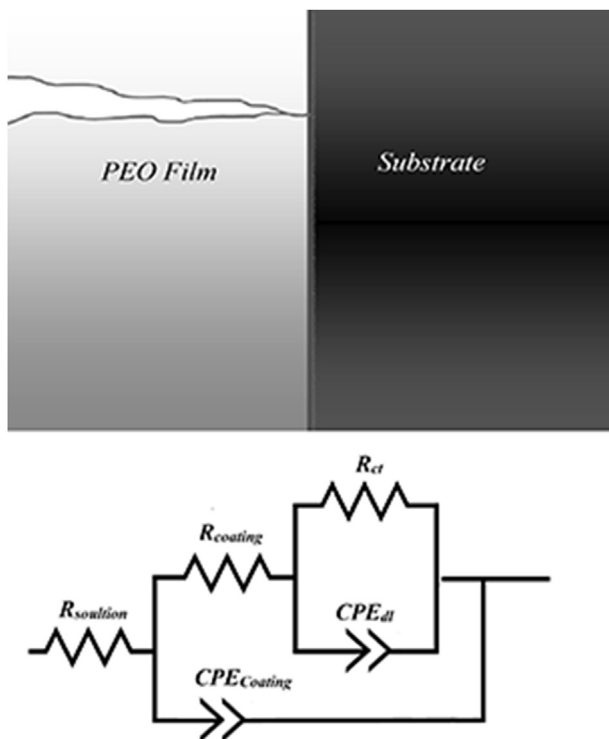
Fig. 7. Schematic presentation of PEO coatings and relevant electrochemical circuit.

phase element is used instead of the capacitor and the proposed formula for calculating the admittance of constant phase element is as follow [48]:

$$Y_{CPE}(\omega) = 1/Z_{CPE} = Q_a(j\omega)^n$$

Bode-phase curves of the coating formed at different concentration of CeO2 are presented in Fig. 8b and demonstrates the fact that the fitting has well implemented. Table 2 represents the results of fitting for electrochemical impedance curves.

As observed, the results apparently show the diameter of nyquist semicircle is increased by adding cerium oxide nanoparticles into the electrolyte, which means increasing of corrosion resistance in the presence of cerium oxide nanoparticles. By comparing Fig. 8 and the results of Table 2, it can be concluded that there is a good accordance between the nyquist plots and calculated data. As it is known from Bode and Bode-phase curves, there are two time constants required to match the results with an equivalent circuit; in which one is related to the coating and another is for electric double layer. As noted, the coating resistance has been increased from 1217 to 12,905 Ω per square centimeter by adding 25 gr/L of cerium oxide nanoparticles. It shows a 10 times increase in corrosion resistance in the presence of cerium oxide nanoparticles in comparison with the sample with no ceria nanoparticles. As discussed in the previous section, improvement of coating's corrosion resistance in the presence of cerium oxide nanoparticles is due to low transmission pathways for invasive ions (such as micro-pores and cracks). As can be seen from Table 2, the values related to n_c is increased with increasing the concentration of ceria oxide nanoparticles. Generally, increasing these values means developing smoother surface with lower roughness [49]. These results are consistent with the results calculated for surface roughness and also in accordance with the results of the SEM micrographs.

3.3. Wear behavior

Coefficient of friction (COF) curve in terms of sliding distance was obtained using the pin-on-disc test with the load of 1 kg and 1800 m distance for the coatings containing different concentrations of cerium oxide and are shown in Fig. 8. Clearly illustrated, in the early distances, the coating with less nanoparticles have lower coefficient of friction and with further sliding the amount of COF related to coated sample at a concentration of 50 gr/L is more than the 0 gr/L. As predicted, the lowest coefficient of friction is of the coated sample at 25 gr/L. The reason for this can be traced back to less roughness of the sample. The general trend of wear test curves is oscillating and the value of these oscillations is less in the sample comprising oxide particles. This means the improvement of wear resistance [37]. The lowest value of oscillations is for the sample
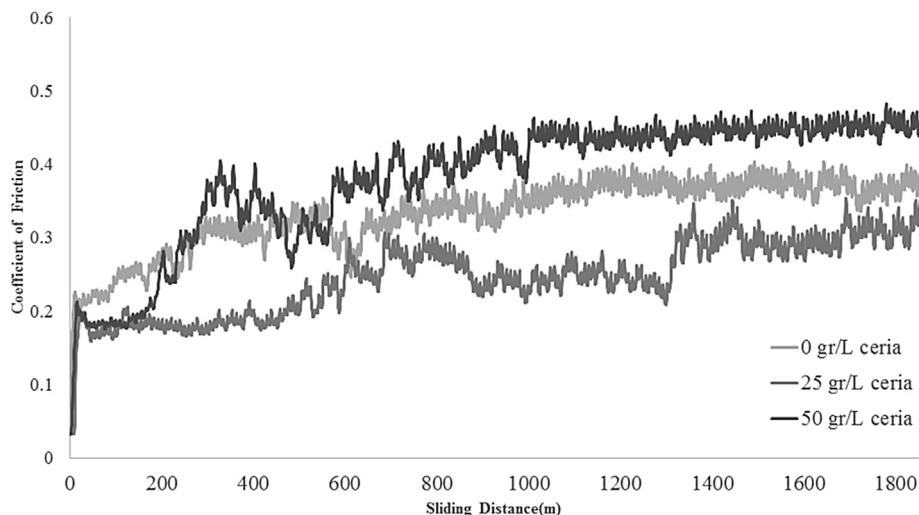
Fig. 8. Coefficient of friction for samples with different ceria concentrations (0, 25, 50 gr/L).

Table 2
Fitting results of EIS tests.

Fitting element	CeO_2 concentration (gr/L)		
	0	25	50
$R_{soultion}$ (ohms)	17.64	18.35	17.04
$R_{Coating}$ (ohms)	1217.1	12905.4	23,231.8
R_{Ct} (ohms)	92,851	1.77E+06	2.72E+06
$CPE_{coating}$ (μF)	83.1	8.36	6.19
$n_{Coating}$	0.666	0.975	0.994
CPE_{dl} (μF)	29.4	1.87	1.81E
n_{dl}	0.816	0.742	0.722
χ^2	0.0046	0. 0053	0.0049

coated at the concentration of 25 gr/L. This specimen before 600 m not only has the lowest COF, but also the fluctuations for this sample are in its lowest value. At this stage, wear is more abrasive [50] and is because of low roughness of the surface [51].

Wear rate curve relative to the concentration of nanoparticles has been shown in Fig. 9. As can be seen, the lowest wear rate is for the sample coated in the concentration of 25 gr/L. According to researches by Aliofkhazraei et al. coating's wear rate has effectively
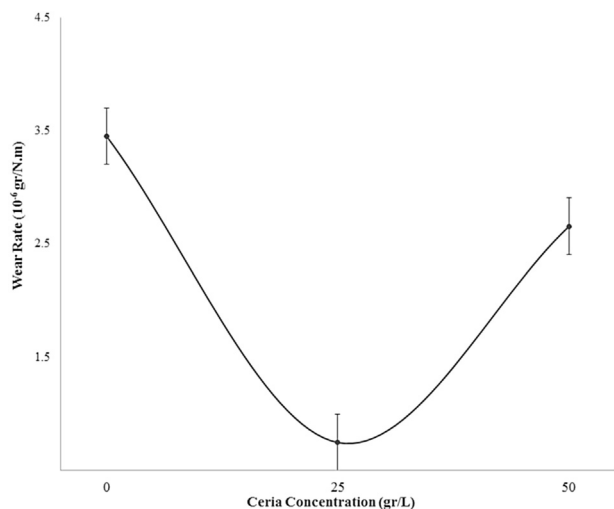

Fig. 9. Wear rate of samples with different ceria concentrations (0, 25, 50 gr/L).

decreased with the addition of hard nanoparticles [43]. Cerium oxide nanoparticles have very high hardness [52,53]. As can be inferred from these results, the wear rate of PEO coating is reduced by adding cerium oxide nanoparticles in the electrolyte. And, the optimal amount for obtaining the best wear resistance is 25 gr/L. This is maybe due to the more roughness created at great concentrations of nanoparticles.

Micrographs of the samples after the wear test are shown in Fig. 10. As can be seen, the presence of ceria nanoparticles in the coating influenced the wear behavior of the coating. Fig. 10 indicates that the coating without ceria nanoparticles has been completely worn after the wear test. The results show that the presence of ceria nanoparticles effectively leads to improvement in wear properties. Unlike the sample without ceria nanoparticles, initial failure in the coating comprising nanoparticles is not considerable. The depth and width of track in the coating containing nanoparticles is less than the nanoparticle-free sample. Coating wear performance can be affected with mechanical properties of the coating material, thickness, surface roughness, porosity and cracks in the coating. Mechanical properties of the coating material are enhanced owing to entering ceria nanoparticles and this can culminate in improving the wear properties of the coating. As was observed in the SEM images, there was defects such as porosity in the coating without nanoparticles that these defects can act as weak points during the wear test. After the entry of nanoparticles into the coating, microstructure of the coating is improved and these structural defects are disappeared. The amount of roughness is also reduced with the addition of nanoparticles into the coating. This also improves the wear behavior. As is clear from Fig. 10, the wear rate has been increased by embedding more nanoparticles into the coating. This phenomenon could be due to increasing porosity and surface roughness amounts of coating because of further increasing of nanoparticles. In general, it is believed that the wear resistance increases by the rise of hardness, specially at the surface [54]. Ceria nanoparticle are hard, so by embedding these hard nanoparticles to the coating, wear resistance of the coating is improved. Increase of coating's wear resistance caused by the entering of nanoparticles into the PEO coating have also been reported by other researchers [55]. Generally, it is believed that the type of wear in PEO coating is of abrasive type and alters to aggravating wear after entering hard nanoparticles [50].
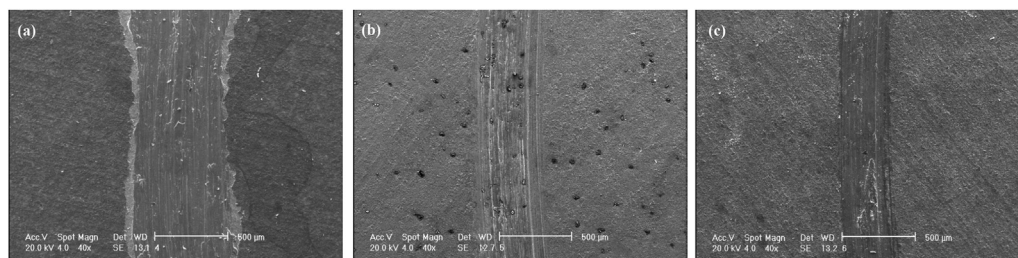
Fig. 10. SEM images of the samples coated in different ceria concentrations after the wear test a) without ceria b) 25 gr/L c) 50 gr/L.

4. Conclusion

In ceria embedded samples, pore dimensions decreased by addition of ceria nanoparticles and some of pores especially in 25 gr/L sample got filled with nanoparticles addition. This yielded in lowest roughness in 25 gr/L concentration and more uniform surface as an optimum condition. Ceria assisted coatings had more noble corrosion potentials, and with addition of ceria concentration, corrosion potential increased, showing more corrosion resistance. Apart from that corrosion current density decreased by addition of ceria nanoparticles into electrolyte. Values for corrosion current density, were similar for both 25 gr/L and 50 gr/L concentrations, but 25 gr/L concentration of nanoparticles in suspension showed lower corrosion current density, due to its more uniform surface and lower porosity. Wear tests showed decrease in coefficient of friction for samples with ceria nanoparticle addition in initial stages, with further wear, friction coefficient of 50 gr/L sample exceeded the nanoparticle-free coatings due to wear of absorbed ceria nanoparticles on surface and lack of incorporation of nanoparticles in depth of coating.

References

[1] T. Falcade, T.E. Shmitzhaus, O.G. dos Reis, A.L.M. Vargas, R. Hübler, I.L. Müller, C. de Fraga Malfatti, Electrodeposition of diamond-like carbon films on titanium alloy using organic liquids: corrosion and wear resistance, Appl. Surf. Sci. 263 (2012) 18–24.

[2] F. Weng, C. Chen, H. Yu, Research status of laser cladding on titanium and its alloys: a review, Mater. Des. 58 (2014) 412–425.

[3] M. Gardon, J. Guilemany, Milestones in functional titanium dioxide thermal spray coatings: a review, J. Therm. Spray Technol. 23 (2014) 577–595.

[4] V. Oliveira, C. Aguiar, A. Vazquez, A. Robin, M. Barboza, Improving corrosion resistance of Ti–6Al–4V alloy through plasma-assisted PVD deposited nitride coatings, Corros. Sci. 88 (2014) 317–327.

[5] Y. Zhu, W. Wang, X. Jia, T. Akasaka, S. Liao, F. Watari, Deposition of TiC film on titanium for abrasion resistant implant material by ion-enhanced triode plasma CVD, Appl. Surf. Sci. 262 (2012) 156–158.

[6] L. Bouchama, N. Azzouz, N. Boukmouche, J. Chopart, A. Daltin, Y. Bouznit, Enhancing aluminum corrosion resistance by two-step anodizing process, Surf. Coatings Technol. 235 (2013) 676–684.

[7] M. Niinomi, Mechanical properties of biomedical titanium alloys, Mater. Sci. Eng. A 243 (1998) 231–236.

[8] S.G. Setti, R. Rao, Tribological behaviour of near β titanium alloy as a function of α+ β solution treatment temperature, Mater. Des. 50 (2013) 997–1004.

[9] R. Schutz, H. Watkins, Recent developments in titanium alloy application in the energy industry, Mater. Sci. Eng. A 243 (1998) 305–315.

[10] M. Pelaez, N.T. Nolan, S.C. Pillai, M.K. Seery, P. Falaras, A.G. Kontos, P.S. Dunlop, J.W. Hamilton, J.A. Byrne, K. O'Shea, A review on the visible light active titanium dioxide photocatalysts for environmental applications, Appl. Catal. B Environ. 125 (2012) 331–349.

[11] J.-H. Kim, A. Ishihara, S. Mitsushima, N. Kamiya, K.-I. Ota, Catalytic activity of titanium oxide for oxygen reduction reaction as a non-platinum catalyst for PEFC, Electrochimica acta 52 (2007) 2492–2497.

[12] S.K. Yazıcı, M. Muhaffel, M. Baydogan, Effect of incorporating carbon nanotubes into electrolyte on surface morphology of micro arc oxidized Cp-Ti, Appl. Surf. Sci. 318 (2014) 10–14.

[13] S. Durdu, M. Usta, The tribological properties of bioceramic coatings produced on Ti6Al4V alloy by plasma electrolytic oxidation, Ceram. Int. 40 (2014) 3627–3635.

[14] S. Tsunekawa, Y. Aoki, H. Habazaki, Two-step plasma electrolytic oxidation of Ti–15V–3Al–3Cr–3Sn for wear-resistant and adhesive coating, Surf. Coatings Technol. 205 (2011) 4732–4740.

[15] M. Shokouhfar, C. Dehghanian, M. Montazeri, A. Baradaran, Preparation of ceramic coating on Ti substrate by plasma electrolytic oxidation in different electrolytes and evaluation of its corrosion resistance: part II, Appl. Surf. Sci. 258 (2012) 2416–2423.

[16] H. Habazaki, S. Tsunekawa, E. Tsuji, T. Nakayama, Formation and characterization of wear-resistant PEO coatings formed on β-titanium alloy at different electrolyte temperatures, Appl. Surf. Sci. 259 (2012) 711–718.

[17] M. Aliofkhazraei, A. Sabour Rouhaghdam, T. Shahrabi, Abrasive wear behaviour of Si3N4/TiO2 nanocomposite coatings fabricated by plasma electrolytic oxidation, Surf. Coatings Technol. 205 (Suppl. 1) (2010) S41–S46.

[18] S. Aliasghari, P. Skeldon, G. Thompson, Plasma electrolytic oxidation of titanium in a phosphate/silicate electrolyte and tribological performance of the coatings, Appl. Surf. Sci. 316 (2014) 463–476.

[19] D. Wei, Y. Zhou, Y. Wang, D. Jia, Characteristic of microarc oxidized coatings on titanium alloy formed in electrolytes containing chelate complex and nano-HA, Appl. Surf. Sci. 253 (2007) 5045–5050.

[20] K.R. Shin, Y.G. Ko, D.H. Shin, Influence of zirconia on biomimetic apatite formation in pure titanium coated via plasma electrolytic oxidation, Mater. Lett. 64 (2010) 2714–2717.

[21] S. Di, Y. Guo, H. Lv, J. Yu, Z. Li, Microstructure and properties of rare earth CeO 2-doped TiO 2 nanostructured composite coatings through micro-arc oxidation, Ceram. Int. 41 (2015) 6178–6186.

[22] B. Valdez, S. Kiyota, M. Stoytcheva, R. Zlatev, J. Bastidas, Cerium-based conversion coatings to improve the corrosion resistance of aluminium alloy 6061-T6, Corros. Sci. 87 (2014) 141–149.

[23] K.C. Tekin, U. Malayoğlu, S. Shrestha, Electrochemical behavior of plasma electrolytic oxide coatings on rare earth element containing Mg alloys, Surf. Coatings Technol. 236 (2013) 540–549.

[24] F. Muhaffel, F. Mert, H. Cimenoglu, D. Höche, M. L. Zheludkevich, C. Blawert, Characterisation and corrosion behaviour of plasma electrolytic oxidation coatings on high pressure die cast Mg–5Al–0.4Mn–xCe (x = 0, 0.5, 1) alloys, Surf. Coatings Technol..

[25] L. Jianzhong, T. Yanwen, G. Zuoxing, Z. Huang, Effects of rare earths on the microarc oxidation of a magnesium alloy, Rare Met. 27 (2008) 50–54.

[26] T.S. Lim, H.S. Ryu, S.-H. Hong, Electrochemical corrosion properties of CeO2-containing coatings on AZ31 magnesium alloys prepared by plasma electrolytic oxidation, Corros. Sci. 62 (2012) 104–111.

[27] X. Cui, Y. Yang, E. Liu, G. Jin, J. Zhong, Q. Li, Corrosion behaviors in physiological solution of cerium conversion coatings on AZ31 magnesium alloy, Appl. Surf. Sci. 257 (2011) 9703–9709.

[28] M. Mohedano, C. Blawert, M.L. Zheludkevich, Cerium-based sealing of PEO coated AM50 magnesium alloy, Surf. Coatings Technol. 269 (2015) 145–154.

[29] T. Seop Lim, H. Sam Ryu, S.-H. Hong, Plasma electrolytic oxidation/cerium conversion composite coatings for the improved corrosion protection of AZ31 Mg Alloys, J. Electrochem. Soc. 160 (2013) C77–C82.

[30] V.S. Rudnev, L.M. Tyrina, I.V. Lukiyanchuk, T.P. Yarovaya, I.V. Malyshev, A.Y. Ustinov, P.M. Nedozorov, T.A. Kaidalova, Titanium-supported Ce-, Zr-containing oxide coatings modified by platinum or nickel and copper oxides and their catalytic activity in CO oxidation, Surf. Coatings Technol. 206 (2011) 417–424.

[31] H. Guo, M. An, H. Huo, S. Xu, L. Wu, Microstructure characteristic of ceramic coatings fabricated on magnesium alloys by micro-arc oxidation in alkaline silicate solutions, Appl. Surf. Sci. 252 (2006) 7911–7916.

[32] E. Matykina, A. Berkani, P. Skeldon, G. Thompson, Real-time imaging of coating growth during plasma electrolytic oxidation of titanium, Electrochimica Acta 53 (2007) 1987–1994.

[33] S. Di, Y. Guo, H. Lv, J. Yu, Z. Li, Microstructure and properties of rare earth CeO2-doped TiO2 nanostructured composite coatings through micro-arc oxidation, Ceram. Int. 41 (2015) 6178–6186.

[34] E. Matykina, R. Arrabal, F. Monfort, P. Skeldon, G.E. Thompson, Incorporation of zirconia into coatings formed by DC plasma electrolytic oxidation of aluminium in nanoparticle suspensions, Appl. Surf. Sci. 255 (2008) 2830–2839.

[35] Z. Yao, Y. Jiang, Z. Jiang, F. Wang, Z. Wu, Preparation and structure of ceramic coatings containing zirconium oxide on Ti alloy by plasma electrolytic oxidation, J. Mater. Process. Technol. 205 (2008) 303–307.

[36] J. Liang, L. Hu, J. Hao, Preparation and characterization of oxide films

containing crystalline TiO 2 on magnesium alloy by plasma electrolytic oxidation, Electrochimica Acta 52 (2007) 4836–4840.

[37] H. Li, Y. Sun, J. Zhang, Effect of ZrO 2 particle on the performance of micro-arc oxidation coatings on Ti6Al4V, Appl. Surf. Sci. 342 (2015) 183–190.

[38] R. Arrabal, E. Matykina, P. Skeldon, G. Thompson, Incorporation of zirconia particles into coatings formed on magnesium by plasma electrolytic oxidation, J. Mater. Sci. 43 (2008) 1532–1538.

[39] E. Matykina, R. Arrabal, P. Skeldon, G. Thompson, Incorporation of zirconia nanoparticles into coatings formed on aluminium by AC plasma electrolytic oxidation, J. Appl. Electrochem. 38 (2008) 1375–1383.

[40] G. Sundararajan, L.R. Krishna, Mechanisms underlying the formation of thick alumina coatings through the MAO coating technology, Surf. Coatings Technol. 167 (2003) 269–277.

[41] X. Li, S. Deng, H. Fu, G. Mu, N. Zhao, Synergism between rare earth cerium(IV) ion and vanillin on the corrosion of steel in H2SO4 solution: weight loss, electrochemical, UV–vis, FTIR, XPS, and AFM approaches, Appl. Surf. Sci. 254 (2008) 5574–5586.

[42] K.M. Lee, K.R. Shin, S. Namgung, B. Yoo, D.H. Shin, Electrochemical response of ZrO 2-incorporated oxide layer on AZ91 Mg alloy processed by plasma electrolytic oxidation, Surf. Coatings Technol. 205 (2011) 3779–3784.

[43] M. Aliofkhazraei, A.S. Rouhaghdam, Wear and coating removal mechanism of alumina/titania nanocomposite layer fabricated by plasma electrolysis, Surf. Coatings Technol. 205 (2011) S57–S62.

[44] M. Schem, T. Schmidt, J. Gerwann, M. Wittmar, M. Veith, G. Thompson, I. Molchan, T. Hashimoto, P. Skeldon, A. Phani, CeO 2-filled sol–gel coatings for corrosion protection of AA2024-T3 aluminium alloy, Corros. Sci. 51 (2009) 2304–2315.

[45] W. Li, D. Li, Influence of surface morphology on corrosion and electronic behavior, Acta Mater. 54 (2006) 445–452.

[46] T.S. Lim, H.S. Ryu, S.-H. Hong, Electrochemical corrosion properties of CeO 2-containing coatings on AZ31 magnesium alloys prepared by plasma electrolytic oxidation, Corros. Sci. 62 (2012) 104–111.

[47] S. Ranganatha, T. Venkatesha, K. Vathsala, Electrochemical studies on Zn/nano-CeO 2 electrodeposited composite coatings, Surf. Coatings Technol. 208 (2012) 64–72.

[48] P. Zoltowski, On the electrical capacitance of interfaces exhibiting constant phase element behaviour, J. Electroanal. Chem. 443 (1998) 149–154.

[49] M.E. Orazem, B. Tribollet, Electrochemical Impedance Spectroscopy, John Wiley & Sons, 2011.

[50] L.R. Krishna, A.S. Purnima, G. Sundararajan, A comparative study of tribological behavior of microarc oxidation and hard-anodized coatings, Wear 261 (2006) 1095–1101.

[51] Y.M. Wang, B.L. Jiang, L.X. Guo, T.Q. Lei, Tribological behavior of microarc oxidation coatings formed on titanium alloys against steel in dry and solid lubrication sliding, Appl. Surf. Sci. 252 (2006) 2989–2998.

[52] S. Kasturibai, G.P. Kalaignan, Characterizations of electrodeposited Ni–CeO 2 nanocomposite coatings, Mater. Chem. Phys. 147 (2014) 1042–1048.

[53] V. Mangam, S. Bhattacharya, K. Das, S. Das, Friction and wear behavior of Cu–CeO 2 nanocomposite coatings synthesized by pulsed electrodeposition, Surf. Coatings Technol. 205 (2010) 801–805.

[54] S.-m. Li, X.-m. Yu, J.-h. Liu, M. Yu, L. Wu, K. Yang, Microstructure and abrasive wear behaviour of anodizing composite films containing SiC nanoparticles on Ti6Al4V alloy, J. Central South Univ. Technol. 12 (2014) 4415–4423.

[55] L. Yu, J. Cao, Y. Cheng, An improvement of the wear and corrosion resistances of AZ31 magnesium alloy by plasma electrolytic oxidation in a silicate–hexametaphosphate electrolyte with the suspension of SiC nanoparticles, Surf. Coatings Technol. 276 (2015) 266–278.